Polarisation vision in the dark: Green-sensitive photoreceptors in the nocturnal ball-rolling dung beetle *Escarabaeus satyrus*

Ayse Yilmaz[1,*], Gregor Belušič[2], James Foster[1,3], Claudia Tocco[1], Lana Khaldy[1], Marie Dacke[1]

[1]Lund Vision Group, Department of Biology, Lund University, 223 62 Lund, Sweden

[2]Department of Biology, Biotechnical Faculty, University of Ljubljana, Večna pot 111, 1000 Ljubljana, Slovenia
[3]Neurobiology, University of Konstanz, Universitätsstr. 10, 78464 Konstanz, Germany

[*]Corresponding author: Ayse Yilmaz, email: ayse.yilmaz-heusinger@biol.lu.se

Keywords: Orientation, polarised light, dung beetle, dorsal rim area, green-sensitive, nocturnal

Summary Statement: The nocturnal dung beetle *Escarabaeus satyrus* uses green-sensitive DRA photoreceptors and a series of morphological adaptations to increase the quality of its celestial compass readings from the night sky.

ABSTRACT

Many insects utilise the polarisation pattern of the sky to adjust their travelling directions. The extraction of directional information from this sky-wide cue is mediated by specialised photoreceptors located in the dorsal rim area (DRA). While this part of the eye is known to be sensitive to the ultraviolet, blue or green component of skylight, the latter has only been observed only in insects active in dim light. To address the functional significance of this, we define the spectral and morphological adaptations of the DRA in a nocturnal ball-rolling dung beetle, the only family of insects demonstrated to orient to the dim polarisation pattern in the night sky.

Intracellular recordings revealed polarisation sensitive green photoreceptors in the DRA of *Escarabaeus satyrus*. Behavioural experiments verified the navigational relevance of this finding. To quantify the adaptive value of green sensitivity for celestial orientation at night, we also obtained the polarisation properties of the night sky in the natural habitat of the beetle. Calculations of relative photon catch revealed that under a moonlit sky the green-sensitive DRA photoreceptors should catch an order of magnitude more photons compared to the UV-sensitive photoreceptors in the main retina. The green-sensitive photoreceptors – which also show a range of morphological adaptations for enhanced sensitivity – provides *E.*

satyrus with a highly sensitive system for the extraction of directional information from the night sky.

INTRODUCTION

As sunlight interacts with small components in our atmosphere, a pattern of linearly polarised light forms across the sky. Many diurnal animals, including fish (Novales Flamarique, 2019), birds (Muheim et al., 2009), spiders (Dacke et al., 2001) and insects (Heinze, 2014; Mathejczyk and Wernet, 2017; Rossel and Wehner, 1984; Rossel et al., 1978; Seidl et al., 2006; Wehner and Müller, 2006; Weir and Dickinson, 2012) extract directional information from this spatially predictable pattern to navigate their environment. A similar pattern of polarised light – albeit up to several million times dimmer – is produced by the moon (Heinze, 2014). This pattern offers a potential directional reference for those that need to find their way at night. To date, only dung beetles (*Scarabaeidae*) are known to steer according to this dimmer version of celestial polarised light (Dacke et al., 2003a; Dacke et al., 2011) but nocturnal species across the animal kingdom may share this ability.

In insects, polarised light is typically detected by two sets of photoreceptors, sharing a common field of view, with orthogonally oriented microvilli along the entire length of the rhabdom (Blum and Labhart, 2000; Homberg and Paech, 2002; Labhart and Meyer, 1999; Labhart et al., 2009; Wernet et al., 2012; Wunderer and Smola, 1982). When used to inform orientation and navigation, these specialised photoreceptors are found in the dorsal most region of the compound eyes, in the so-called dorsal rim area (DRA). Additional anatomical specialisations such as widened and shortened rhabdoms – to enlarge receptive fields and reduce self-screening, respectively – enhance the sensitivity to polarised light (reviewed in (Labhart and Meyer, 1999)).

The spectral sensitivity of DRA photoreceptors varies across species. The DRAs of honeybees (Labhart, 1980), bumblebees (Meyer-Rochow, 1981), ants (Labhart, 1986), flies (Fortini and Rubin, 1991; Wernet et al., 2003), butterflies (Stalleicken et al., 2006) and diurnal dung beetle species (Dacke et al., 2002; Khaldy et al., 2022) are equipped with photoreceptors primarily sensitive to the ultraviolet (UV) component of light. This widespread perception of celestial polarised light in the UV is rather counterintuitive, as both the degree of linear polarisation and the intensity of the light from the clear sky are considerably lower in the UV than in the blue or green region of the spectrum (Barta and Horváth, 2004; Brines and Gould, 1982; Coulson, 1988). However, the shorter the

wavelength, the greater the proportion of celestial polarisation that can be used by animals under cloudy-sky conditions (Barta and Horváth, 2004; Brines and Gould, 1982; Pomozi et al., 2001). The UV-sensitive DRAs of diurnal insects are thus likely adapted to also support the perception of the celestial polarised light pattern under cloudy conditions. While blue-sensitive DRA photoreceptors can be found in crickets (Labhart et al., 1984; Zufall et al., 1989), desert locusts (Eggers and Gewecke, 1993; Schmeling et al., 2014) and cockroaches (Loesel and Homberg, 2001), green-sensitive photoreceptors have so far been reported only for beetles (Bisch, 1999; Khaldy et al., 2022; Labhart et al., 1992) and moths (Belusic et al., 2017). The nocturnal activity of many of these insects suggests that the sensitivity to polarised light in the blue or green spectrum of light is an adaptation to the perception of the celestial polarisation pattern during the darker hours of the day (Hegedüs et al., 2006; Herzmann and Labhart, 1989; Homberg et al., 2011), but the functional significance of this warrants further investigation.

To steer across the savanna, the nocturnal dung beetle *Escarabaeus satyrus* (Boheman, 1860) extracts directional information from the moon, the stars and the pattern of polarised light that spans the night sky (Dacke et al., 2004; Dacke et al., 2011; Dacke et al., 2013). This beetle's relatively large eyes can be expected to support a high sensitivity to light (Byrne and Dacke, 2011; Tocco et al., 2021), but the specific adaptations that enable these insects to perceive the dim polarisation patten of the night sky has not been well described. To address this, we first characterised the spectral sensitivity of the photoreceptors in the DRA of the beetle and confirmed its navigational relevance. To understand the adaptive value of green spectral sensitivity for the analysis of the celestial polarisation pattern, we also obtained the polarisation properties of the blue and green components in the South African night sky in the natural habitat of the beetle. A characterisation of the relative photon catches from a night sky for the green-sensitive receptors in the DRA and the UV-sensitive receptors of the main retina (that also contained green-sensitive photoreceptors), revealed that green-sensitive DRA photoreceptors should catch an order of magnitude more photons from the night sky compared to UV-sensitive photoreceptors in the main retina. Finally, we also identified a range of morphological adaptations in the DRA of *E. satyrus* for increased sensitivity to light.

MATERIALS AND METHODS

Animals

Nocturnal ball-rolling dung beetles, of the species *Escarabaeus satyrus*, were collected at Stonehenge game farm (24.32°E, 26.39°S) in South Africa and transported to Lund

University, Sweden. Here the beetles were kept in large soil-filled plastic bins in a climate-controlled room (at 26°C and a 12h light:12h dark regime) and fed with fresh horse dung *ad libitum*.

Histology

Extracted beetle eyes were fixed for 48h with 2% paraformaldehyde, 2% glutaraldehyde, 0.1 mmol EGTA and 0.1 mmol sucrose in 0.1 mol sodium cacodylate buffer (pH 7.2) at room temperature. The samples were then processed through a series of washes in sodium cacodylate buffer and post-fixated in 1% OsO_4 in distilled H_2O at 4°C for 2.5h. This was followed by a dehydration process in an increasing ethanol (70% 2 x 10 min; 96% 2 x 10 min; > 99% 2 x 15 min) and acetone (acetone 2 x 20 min; 2:1 acetone/epon 1 x 30 min; 1:1 acetone/epon overnight) series, and transfer to and embedding in fresh Epoxy resin. Semi-thin (1 µm) and ultra-thin (50 nm) sections of the eye (RMC Powertome PT XL, Boeckeler, USA) were stained with toluidine blue (for light microscopy; Axiophot, Zeiss, Germany) or 1% uranyl acetate and lead citrate (for electron microscopy; JEM-1400plus, Japan). For scanning electron microscopy (Hitachi, SU3500, US), the beetles were air-dried and sputter-coated with gold–palladium (40/60).

Photoreceptor recordings

Spectral sensitivity

The beetles were cold-anaesthetised, immobilised with beeswax and resin and mounted on a goniometric XYZ-stage that carried a micromanipulator (Sensapex, Oulu, Finland). Microelectrodes, pulled from 1 mm diameter borosilicate capillaries on a horizontal puller P-2000 (capillaries and puller Sutter, Novato, CA, USA) were filled with 3 mol l^{-1} KCl (resistance 100–150 MΩ) and inserted into the photoreceptors of the expected polarisation-sensitive dorsal rim area region through a small triangular hole in the cornea of the dorsal eye. A 50 µm diameter Ag/AgCl reference electrode was inserted into the head capsule next to the eye. The beetles were kept in darkness for 20 min at room temperature prior to the recordings. The electric signal was amplified (SEC 10 LX amplifier, Npi electronic, Tamm, Germany; Cyber Amp 320, Axon Instruments, Union City, CA, USA) and digitised (Micro 1401, CED, Cambridge, UK). Spectral stimulation was provided with an LED array ('LED synth'(Belušič et al., 2016)) or a xenon arc lamp (XBO, Cairn Research Ltd, Faversham, UK) filtered with a monochromator (B&M, Limburg, Germany) tuned to emit equal numbers of

photons (max. 10^{15} quanta s^{-1} cm^{-2} at 10 nm bandwidth) at all wavelengths ('isoquantal' mode).

Polarisation sensitivity (PS)

A quick stimulation with the LED synth allowed for an initial categorisation of the spectral sensitivity of the cell (peak at 365 or 520 nm). An intensity-response series and a sequence of responses to polarised light were recorded at the peak sensitivity wavelength. Polarised light was created by shining monochromatic light through a polarisation filter (OUV2500, Knight Optical, Harrietsham, UK) mounted on a motorised rotator (Qioptiq, Göttingen, Germany). Next, for the cells held for 6 min or more (n=31), a detailed spectral scan with the monochromator (see above) was performed. The spectral responses and responses to polarised light were transformed to sensitivity by means of an intensity–response function and a reverse Hill transformation (Belusic et al., 2017). A $\cos^2$ function was fitted to the polarisation sensitivity data and PS ratio of the photoreceptors was calculated as the ratio between the function maximum and minimum, i.e. $PS=S_{max}/S_{min}$ (Bernard and Wehner, 1977).

Receptive field size

The impaled green-sensitive cells were oriented towards a back-projection screen (ST-Pro-X, Screen-Tech e.K., Hohenaspe, Germany) and stimulated with a DLP (digital light processing) projector (LightCrafter 4500, Texas Instruments, USA) emitting light at ~530 nm at 220 Hz refresh rate. The receptive field centre was first located at the maximal response coordinates upon the passage of a horizontal and vertical bar across the screen. The cells were then stimulated with 1.4°×1.4° green square stimuli, flashing on a 26.6°×26.6° grid. The stimulus was generated with PsychoPy software (Peirce et al., 2019). Voltage responses were transformed into sensitivity, normalised and the resulting 2D spatial sensitivity matrix was fitted with an ellipsoid 2D-Gaussian curve with three free parameters – standard deviations ($\sigma_{1,2}$) and maximal radius angle – yielding two acceptance angles ($\Delta\rho_{1,2}$), calculated as the full width at half maximum $\Delta\rho_{1,2} = 2.355\ \sigma_{1,2}$.

Photoreceptor excitation calculations

To calculate the relative photon catch of green-sensitive photoreceptors in the DRA and green- and UV- sensitive photoreceptors in the main retina – at different regions of the spectrum, we used the defined spectral sensitivities of each photoreceptor and irradiance spectra of sunlit, moonlit and starlit skies as reported by Johnsen et al. (Johnsen et al., 2006).

Behaviour

Experimental set-up

Twenty-one circularly arranged light-emitting diodes (LEDs) with a maximum emission peak at 520 nm (Lumileds, San Jose, CA, USA) were mounted on a square-shaped aluminium plate (60 x 60 cm) placed 60 cm above a 60 cm diameter sand-painted circular arena (Fig. 1A, see also (Khaldy et al., 2022)). To diffuse the light, 10 sheets of sandblasted plexiglass (60×60×0.3 cm, Plexiglas® Solar 2458, EBLA-GmbH, Appenweier, Germany) were placed at 1 cm intervals starting from 7.5 cm below the LEDs. A 60 cm diameter polarisation filter (BVO UV Polarizer, Bolder Vision Optik©, Boulder, CO, USA) was placed below the 10th sheet of Plexiglas. The intensity of the 100% linearly polarised green light was adjusted by neutral density filters (LEE filters) placed in between the LED layout and diffusers to a photon flux of $6x10^{8}$ photons $cm^{-2}s^{-1}$ (resembling the irradiance of green spectrum of a moonlit sky (Johnsen et al., 2006) as measured from the centre of the arena (QE65000; Ocean Optics, Dunedin, FL, USA).

Experimental procedure

A beetle was placed alongside its dung ball in the centre of the circular arena and allowed to roll its ball to the arena perimeter. Here, the exit bearing was noted, the beetle was removed from its ball and placed back to the center of the arena with its ball. This procedure was repeated another four times, resulting in five exits per beetle. Beetles for which the angular distribution of the first five exit angles did not differ from a uniform distribution ($P > 0.1$, Rayleigh test on axial data) were excluded from further experimentation. This allowed us to identify beetles that were motivated to orient under the highly artificial experimental conditions presented to them. Each beetle that passed this test was allowed to exit the arena an additional five times, resulting in 10 exits per beetle. After the fifth exit, the linear polarisation filter was either turned by 90° (*test*) or kept in place (*control*) (Fig. 1A). The initial orientation of the overhead polarisation filter was alternated between an e-vector alignment of 0° - 180° and 90° - 270° with respect to the 0° mark on the circular arena.

Data analysis

The initial bearing selection of the population in relation to the e-vector of light was obtained from each beetle's first exit-point under the polarisation filter (Fig. 1B). A Rayleigh´s uniformity test for axial data was used to test for uniformity of the distribution (Batschelet, 1981). The angular response to a 90° rotation of the overhead polarisation filter (*test*), was

calculated from the differences of the mean bearing for exits 1-5 and the mean bearing for exits 6-10 for each beetle. As a *control*, the corresponding angular change in direction (between the mean bearing for exits 1-5 and the mean bearing for exits 6-10) was obtained for beetles exiting the arena when the polarisation filter remained in place. A V-test for axial data was applied with an expected mean of 0°-180° for the *control* group and 90°-270° for the *test* group. Circular statistics were performed using Oriana 4.0 (Kovach Computing Services, Anglesey, UK).

Sky measurements

Skylight polarisation data was adapted from (Foster et al., 2019). An image series was recorded through a photographic polariser (WR 72mm: Sigma) with the transmission axis oriented 0°, 45°, 90°, 135° and 180° to the image's horisontal axis. This series was repeated in five directions for each sky condition: towards the zenith, as well as North, East, South and West towards the horizon. The image series were stitched together to create a single full-sky image and converted to estimated absolute spectral radiance for the camera's red, green and blue colour channels. The same image was also convolved with a 7° half-width Gaussian filter to approximate the receptive fields measured for DRA photoreceptors (Fig. 6A). For the blue channel (as a proxy for short wavelengths more generally (Pomozi et al., 2001)) and the green channel, which matches well with the spectral sensitivity of *E. satyrus'* DRA photoreceptor, pixel-wise polarisation was compared across a full moon, waning gibbous moon and waxing quarter moon recorded at the location where the beetles were collected.

RESULTS

A large dorsal rim area (DRA) with longer rhabdoms

The superposition compound eyes of *E. satyrus* are positioned on each side of the head and divided by a cuticular ridge, the canthus, into two dorsal eyes and two larger ventral eyes (Fig. 2A). The surface of the dorsal eyes is smooth without any external visual borders between the facets. The thick corneal lens of each ommatidium is followed by a crystalline cone, the clear zone and the light sensitive retina (Fig. 2C,F). Serial cross-sectioning through the retina revealed two types of rhabdoms. In the dorsalmost 30 % of the dorsal eye (505 ± 37 ommatidia, n=2), the microvilli of seven untwisted retinular cells form a heart-shaped rhabdom with the microvilli of one of the seven rhabdomeres oriented perpendicular to that of the other six (Fig. 2 D). In other dung beetle species, and in insects in general, this type of orthogonal arrangement is well known to support polarisation vision (Dacke et al., 2003b),

and its full extension over the dorsal part of the eye is termed the dorsal rim area (DRA) (Labhart and Meyer, 1999). In the remaining 72 % of the dorsal eye (ca. 1200 ommatidia, n=2), the microvilli of the seven retinular cells instead diverge in different directions, forming a flower-shaped rhabdom (Fig. 2D). The rhabdoms in the DRA are longer (106.1 ± 8.5 μm, mean ± s.d., t-test, $p < 0.001$, n=9) and somewhat wider (12.3 ± 2.1 μm) than those in the rest of the eye (82.6 ± 4.6 μm and 10.2 ± 0.3 μm, respectively (Fig. 2B,F, 3A, B). This results in rhabdomeric volumes almost twice as large (assuming a cylindrical shape) in DRA retina as in the main retina; 1.3 x 10^4 mm^3 vs. 6.9 x 10^3 μm^3 (Fig. 3C). In *E. satyrus*, the rhabdoms are not optically isolated from each other by screening pigments (Fig. 2C,D,E). Instead, they are partly surrounded by reflective sheath that extend to 34.2% of the length of the rhabdom in the DRA, but as far as to 72.1% of the length of the rhabdom in the main retina (35.0 ± 8.3 μm vs 59.2 ± 4.0 μm in height, t-test, $p < 0.0001$) (Fig. 2E, F, Fig. 3A). When the cornea and the clear zone were experimentally removed from the eye, the uppermost dorsal part of the dorsal eye appeared darker than the main retina (Fig. 2B). This optical effect is likely due to the relatively shorter tracheal sheath of the DRA and thus serves as a good, visual indicator of the same.

The light sensitivity of a photoreceptor can be estimated using the equation

$$S = \left(\frac{\pi}{4}\right)^2 A^2 \left(\frac{d}{f}\right)^2 \left(\frac{kl}{2.3 + kl}\right)$$

where A is the superposition aperture (not measured in this study), f the focal length, i.e. posterior nodal distance (Land, 1997), k the absorption coefficient, and d and l are the diameter and length of the rhabdom, respectively (Warrant and Nilsson, 1998). Assuming that all parameters except d and l are equal between the DRA and the main retina, the longer and wider receptors in the DRA can – according to our defined parameters - be expected to be at least 1.6 times more sensitive to broadband white light than the receptors in the main retina.

The DRA shows high polarisation sensitivity in the green part of the light spectrum.

Intracellular photoreceptor recordings in the DRA of *E. satyrus* revealed one photoreceptor class, maximally sensitive to light in the green part of the spectrum ($\lambda_{max} \approx$ 520 nm, n = 7) (Fig. 4A). Recordings in the main retina rather indicated two types of spectrally distinct photoreceptors, one maximally sensitive to the ultraviolet (UV, $\lambda_{max} \approx$ 365 nm, n = 3) and one to the green ($\lambda_{max} \approx$ 520 nm, n = 8) part of the spectrum (Fig. 4B). The green-sensitive photoreceptors in the DRA and the main retina both had a slightly broader spectral sensitivity

compared to the opsin template with λ_{max} = 520 nm, and a β-peak of sensitivity in the UV range with a variable amplitude (5–45% relative to the peak at 520 nm) (Fig. 4A,B). As expected from their rhabdomeric structure (Fig. 2E), the green-sensitive photoreceptors in the DRA were found to have a higher polarisation sensitivity (PS=7.3 ± 5.7; mean ± s.d., n = 16) than the photoreceptors in the adjacent main retina (PS=1.2 ± 0.2, n = 15) (Fig. 4C,D). The observed variability in polarisation sensitivity values can most likely be ascribed to varying sizes of the targeted rhabdomeres (Immonen et al., 2014), as well as retinal depths and the proximity of the recording site to the lamina where the recordings were obtained. For the UV-sensitive photoreceptors of the main retina, a tail of sensitivity (less than 5% relative to the peak at 365 nm) could be observed between 400 and 600 nm (Fig. 4B).

The receptive fields of the photoreceptors were elliptical and could be described with two angular radii, $w_{1,2}$. The radii in the DRA (w_1=6.4 ± 0.7°; w_2=7.5 ± 0.9°, n = 5) did not differ significantly in length from the radii (w_1=5.9 ± 0.5°; w_2=7.4 ± 0.8°, n = 8) in the green-sensitive photoreceptors in the main retina (t test, p_{w1}=0.25, p_{w2}= 0.95) (Fig. 4E,F).

E. satyrus can detect and orient to the polarised light in the green region of the spectrum.

When repeatedly released with their dung-balls in the centre of the circular experimental arena under highly linearly polarised green light (λ_{max}= 520 nm), the beetles tended to preferentially exit along bearings roughly aligned with the e-vector of the overhead light source (mean, 95% CI: 15.1°, 359.4° - 30.9°, p = 0.003, n=15, Rayleigh test) (Fig. 1B). The 10 exit bearings recorded for each beetle also revealed a directed bimodal distribution (r_{axial} = 0.63 ± 0.15, n=30). When the filter was maintained in the same position for the two sets of five consecutive exits (Fig. 5A), the angular change of direction was only $6.2°_{axial}$ (95% CI: 335.1° - 37.3°, p = 0.025, V-test for axial data along the 0°-180° axis, n=15). In contrast, when the filter was rotated by 90° after the first five exits (Fig. 5B) the angular changes of direction between the mean bearing of exits 1-5 vs exits 6-10 (Fig. 5A) resulted in a mean angular response of 108.9_{axial} (%95 CI: 92.4° - 125.2°, p < 0.001, V-test for axial data along the 90-270° axis, n=15) (Fig. 5B). This change in bearing is significantly different to the control condition where the polariser remained in the same position (p=0.003, Mardia-Watson-Wheeler Test). Overall, these results clearly demonstrate that the nocturnal dung beetle *E. satyrus* can detect and orient to polarised light in the green region of the spectrum.

Sky measurement

Skylight polarisation measurements for a moonlit sky (Fig. 6) close to a full moon revealed that, while the distributions of per-pixel degree of polarisation for the green and blue channels overlapped closely, modal values, representing the high degree of polarisation band, were slightly shifted towards lower values for the green channel as compared to the blue channel (0.60 and 0.65 respectively) (Fig. 6B). Similarly, a notable shift towards lower degrees of polarisation for the green channel compared to the blue channel was observed for the higher-elevation 93%-illuminated waning gibbous moon (modal values of 0.57 and 0.60) (Fig. 6C). The reduced moon fullness during the first quarter resulted in generally lower degrees of polarisation across the sky (Fig. 6D). In this case, the modal degree of polarisation around 0.15 for the green channel was close to the reported threshold for *E. satyrus* (Foster et al., 2019).

Calculations of relative photon catch for the green-sensitive photoreceptors in the DRA and the UV-sensitive photoreceptors in the main retina revealed that the green-sensitive photoreceptors would catch an order of magnitude more photons compared to the UV-sensitive photoreceptors under moonlit conditions (relative photon catch 9.26×10^{10} vs 9.78×10^{9} quanta per receptor) (Fig. 7). This holds true also under the day sky (relative photon catch 6.28×10^{13} vs 8.95×10^{12} quanta per receptor) and a starlit sky on a moonless night (relative photon catch 1.96×10^{8} vs 4.48×10^{7} quanta per receptor) (Fig. 7).

DISCUSSION

The dorsal rim area of *Escarabaeus satyrus* is highly sensitive to polarised light

The upper third of the dorsal eye in *E. satyrus* is internally characterised by heart-shaped rhabdoms, formed by two orthogonally arranged groups of retinal cells with straight and aligned microvilli (Fig. 2). This microvillar arrangement, that supports an analysis of the direction of the e-vector of light, decoupled from its intensity, is a common characteristic of visual systems sensitive to the polarisation of light (Labhart and Meyer 2002; Nilsson et al. 1987; Labhart, 2016). Intracellular recordings from the photoreceptors in the upper third of the retina of *E. satyrus* also revealed a polarisation sensitivity (PS) of ≈ 7 (Fig. 4C). Polarisation sensitivities comparable to that of *E. satyrus* have also been identified in crepuscular crickets (PS ≈ 8.3) (Labhart et al., 1984) and dung beetles (PS ≈ 7.7) (Dacke et al., 2003b), as well as in a range of diurnal insects including honeybees (PS ≈ 6.6) (Labhart,

1980), monarch butterflies (PS ≈ 9.4) (Stalleicken et al., 2006) and ants (PS ≈ 6.3) (Labhart, 1986).

The flower shaped rhabdoms in the rest of the eye of *E. satyrus* are composed of retinular cells with a wide range of microvillar directions. As observed for similar cellular morphologies in other species, the polarisation sensitivity in this part of the eye is drastically reduced (PS ≈ 1.2) (Fig. 4E). Our results thus indicate that the DRA of *E. satyrus* provides the anatomical and physiological substrate for their documented ability to extract directional information from the nocturnal celestial polarisation pattern (Dacke et al., 2011).

The DRA of *Escarabaeus satyrus* is morphologically adapted to increase photon catch

The low intensity of lunar skylight presents a challenge for the perception of the celestial polarisation pattern at night, and the DRA of *E. satyrus* shows a range of morphological adaptations to meet this challenge (Fig. 2). The larger rhabdomeric volume (twice as large in the DRA compared to the rest of the eye) should increase the light sensitivity of the polarisation-sensitive receptors (Labhart et al., 1992) and improve the signal to noise ratio (Heras and Laughlin, 2017). DRAs with relatively longer rhabdoms compared to the rest of the eye have also been described in the dim-light active dung beetle *S. zambesianus* (Dacke et al., 2003b), the cockchafer *Melolontha melolontha* (Labhart et al., 1992) and in crickets (Burghause, 1979). In contrast, the rhabdoms of the DRA photoreceptors in other polarisation sensitive insects are often shorter than those of the main retina (Labhart and Meyer, 1999; Nilsson et al., 1987). For example, in the diurnal ant *Cataglyphis bicolor*, the DRA rhabdoms are significantly shorter (70-75 μm) than the rhabdoms (120 μm) of the main retina (Herrling, 1976). Shorter rhabdoms favour polarisation sensitivity through reduced self-screening (Heinze, 2014; Labhart and Meyer, 1999; Nilsson et al., 1987), but for the analysis of the dim celestial pattern of polarised light in the night sky, the extra absorption by longer rhabdoms apparently outcompetes this effect.

The rhabdoms in the dorsal eyes of *E. satyrus* are partly isolated from each other by tracheal sheath (Fig. 2F). These light scattering structures – that are relatively shorter in the DRA compared to the rest of the eye – also act to increase the overall sensitivity of the photoreceptors by repeatedly reflecting incident light through the rhabdoms (Labhart et al., 1992; Warrant and McIntyre, 1991). In butterflies, these internal reflections only slightly depolarise the reflected light (Nilsson and Howard, 1989). However, the tapetum in eyes with superposition optics is different from that in butterflies and creates a mirrored box around the rhabdom. This box-like organisation of the shorter tracheal sheath in the DRA of *E. satyrus* might depolarise the incident light to a higher degree. Thus, the shorter tracheal

sheath in the DRA is likely the result of a trade-off between an adaptation to enhance sensitivity, while maintaining a high degree of polarisation of incident light.

The resultant receptive fields of DRA photoreceptors, defined as 6.4° (Fig. 4E), are, not significantly larger than the 5.9° defined for the main retina of the dorsal eye. Although not directly addressed in this study, the unusually large DRA with ca. 500 ommatidia covering 30 % of the dorsal eye of the beetle (Fig. 2B), opens for the possibility of extensive spatial summation of the polarisation signal, for increased sensitivity, but again at the cost of spatial resolution (Greiner et al., 2005; Hardcastle et al., 2021; Kind et al., 2021; Klaus and Warrant, 2009; Sancer et al., 2019; Theobald et al., 2007). However, for the specific task of extracting directional information from the night sky, lower spatial resolution might be a benefit rather than a cost. This is because larger sampling units effectively reduce the effect of disruption in the celestial polarisation pattern caused by aerosols and clouds by removing the noise in finer spatial details (Labhart, 1999; Labhart et al., 2001). The crepuscular dung beetle *S. zambezianus* and the nocturnal cockchafer *M. melolontha* also holds large DRAs with ca. 500 (calculated from (Dacke et al., 2003b) and ca. 280 (calculated from (Labhart et al., 1992) ommatidia, respectively. The DRA is much less prominent in the nocturnal bee *Megalopta genalis* (Greiner et al., 2007), the nocturnal ant *Myrmecia pyriformis* (Reid, 2010) and the nocturnal corn borer moth *Ostrinia nubilalis* (Belusic et al., 2017), as the DRA of these insects consist of ca. 140, 120 and 100 ommatidia and covers only ca. 2.4%, 1.7% and 3% of their eye respectively.

The DRA photoreceptors are primarily sensitive to the green spectrum of light

The photoreceptors in the DRA of *E. satyrus* are sensitive to a broad spectral range - from green to UV – with a peak in the green (520 nm) (Fig. 4A). To confirm the navigational relevance of this spectral sensitivity of the DRA photoreceptors, the beetles were allowed to orient under a linearly polarised artificial sky of this wavelength. The beetles did indeed orient with high precision under the green light, but preferentially along bearings that coincided with the e-vector of the artificial sky (Fig. 5B). In crickets, this type of polarotactic behaviour is induced when the animal, as in this study, is presented with a stimulus of a high degree of polarisation (Brunner and Labhart, 1987; Henze and Labhart, 2007). Earlier laboratory experiments reveal that *E. satyrus* can also orient to polarised light in the UV range of the spectrum (Foster et al., 2019). In this case, the perception of UV polarised light is most likely mediated through the secondary absorbance peak (β-band) of the green-sensitive DRA photoreceptors, but we cannot fully exclude the possibility that there is a small proportion of UV-sensitive photoreceptors in the DRA that escaped our recordings. It is

worth noting that in Foster et al., (2019) the intensity level used to elicit a response to polarized UV light was three orders magnitude brighter than the UV content typically present in the moonlight sky (Johnsen et al., 2006).

The two types of photoreceptors in the main retina, one maximally sensitive to the green ($\lambda_{max} \approx 520$ nm) and one maximally sensitive to the UV ($\lambda_{max} \approx 365$ nm) range of the spectrum suggest a physiological substrate for a UV-green dichromatic colour vision system, as has been suggested in many other beetle species (Sharkey et al., 2017; Wu et al., 2020; Yilmaz et al., 2022). Considering that the opsin genes typically sensitive to "blue" wavelengths were lost prior to the origin of modern beetles, approximately 300 million years ago, the identified sensitivity peaks in green and UV – but not in the blue - did not come as a surprise (Sharkey et al., 2017). The UV-sensitive photoreceptors typically exhibit response thresholds approximately one log unit lower than the green-sensitive photoreceptors (Fig. 7). This corresponds well to the lower availability of UV photons compared to the green photons. This balance of response thresholds against the spectrum of ambient illumination could potentially be important in color vision.

Biological significance of different photoreceptor types in the DRA for the analysis of the polarisation pattern in the night sky

The dry semi-arid habitats of *E. satyrus* regularly provide the beetles with clear night skies with celestial patterns of high degrees of polarisation (Foster et al., 2019). The radiance of the moonlit sky in the $green_{500\text{-}600nm}$ part of the spectrum is 14 % higher than in the $blue_{400\text{-}500nm}$ and 68 % higher than in the $UV_{300\text{-}400nm}$ (calculated from (Johnsen et al., 2006); see also (Foster et al., 2019)). That is, at night, there are relatively more photons available in the longer wavelengths of light. Indeed, this is also the primary part of the spectrum that underlies polarisation vision in *E. satyrus*. This stands in direct contrast to diurnal dung beetle species, which – like most day active navigators - rely primarily on the more robust ultraviolet (UV) component of the celestial polarisation pattern (Dacke et al., 2002; Khaldy et al., 2022). This indicates that, for the analysis of the dim celestial pattern of polarised light in the night sky, the benefits of the higher absorption of light in the green outcompetes the challenges imposed by the larger depolarizing effect of clouds in these longer wavelengths of light (Seliger et al., 1994). While the blue sensitive DRA photoreceptors of crickets support the detection of celestial polarised light under partly cloudy skies as well as during twilight and at night (Henze and Labhart, 2007; Herzmann and Labhart, 1989), the large green-sensitive DRA of *E. satyrus* seems to be built to primarily meet the challenge of low light intensities and allows the nocturnal beetles to orient with the same precision as their diurnal

relatives even under crescent moon conditions (Dacke et al., 2011). In addition, as star light spectrum has peaks in the green region of the spectrum (Johnsen et al., 2006), the green-sensitive photoreceptors of the unusually large DRA of *E. satyrus* could, in theory, also support their documented orientation to the Milky Way (Foster et al., 2018).

In summary, green-sensitive DRA photoreceptors, together with a range of morphological adaptations for increased sensitivity, allow the nocturnal ball-rolling dung beetle *E. satyrus* beetles to increase the quality of their celestial compass readings from the night sky throughout the lunar cycle.

Authors' contributions

A.Y.: conceptualization, investigation; analysis, visualization, data curation, writing the first draft, writing, review, and editing; G.B.: investigation, analysis, review, and editing; JJF: investigation, visualization, analysis, review, and editing, C.T.: investigation; L.K.: investigation, M.D.: conceptualization, funding acquisition, resources, writing, review, and editing. All authors: final version of manuscript.

All authors gave final approval for publication and agreed to be held accountable for the work performed therein.

Acknowledgements

The authors are grateful to Willi Ribi at the Australian National University for kindly providing the cross-section images of the retina in Fig. 2D,E, Carina Rasmussen for assistance in obtaining the EM and light microscopy data and Marcus Byrne at the University of the Witwatersrand for assistance in collecting the beetles.

Funding

This work was supported by the European Research Council (817535-UltimateCOMPASS, M.D.), the Air Force Office of Scientific Research (grant no. FA9550-19-1-7005, G.B.), Javna Agencija za Raziskovalno Dejavnost RS (grant no. P3-0333, G.B.) and DFG (project no. 451057640, J.J.F.).

Competing interests:

The authors declare no competing interests.

REFERENCES

Barta, A. and Horváth, G. (2004). Why is it advantageous for animals to detect celestial polarization in the ultraviolet? Skylight polarization under clouds and canopies is strongest in the UV. *J. Theor. Biol.* **226**, 429–437.

Batschelet, E. (1981). Circular Statistics in Biology. *Acad. Press*.

Belusic, G., Sporar, K. and Meglic, A. (2017). Extreme polarisation sensitivity in the retina of the corn borer moth Ostrinia. *J. Exp. Biol.* **220**, 2047–2056.

Belušič, G., Ilić, M., Meglič, A. and Pirih, P. (2016). A fast multispectral light synthesiser based on LEDs and a diffraction grating. *Sci. Rep.* **6**, 1–9.

Bernard, G. D. and Wehner, R. (1977). Functional similarities between polarization vision and color vision. *Vision Res.* **17**, 1019–1028.

Bisch, S. M. (1999). Orientierungsleistungen des nachtaktiven Wustenkafers Parastizopus armaticeps Peringuey (Coleoptera: Tenebrionidae).

Blum, M. and Labhart, T. (2000). Photoreceptor visual fields, ommatidial array, and receptor axon projections in the polarisation-sensitive dorsal rim area of the cricket compound eye. *J. Comp. Physiol. - A Sensory, Neural, Behav. Physiol.* **186**, 119–128.

Brines, M. L. and Gould, J. L. (1982). Skylight polarization patterns and animal orientation. *J. Exp. Biol.* **96**, 69–91.

Brunner, D. and Labhart, T. (1987). Behavioural evidence for polarization vision in crickets. *Physiol. Entomol.* **12**, 1–10.

Burghause, F. M. H. R. (1979). Die strukturelle Spezialisierung des dorsalen Augenteils der Grillen (Orthoptera, Grylloidea). *Zool. J. Physiol* **83**, 502–525.

Byrne, M. and Dacke, M. (2011). The Visual Ecology of Dung Beetles. In *Ecology and Evolution of Dung Beetles*, pp. 177–199.

Coulson, K. L. (1988). Polarization and intensity of light in the atmosphere. *Hampton,VA, USA.*

Dacke, M., Doan, T. and O'Carroll, D. (2001). Polarized light detection in spiders. *J. Exp. Biol.* **204**, 2481–90.

Dacke, M., Nordström, P., Scholtz, C. H. and Warrant, E. J. (2002). A specialized dorsal rim area for polarized light detection in the compound eye of the scarab beetle Pachysoma striatum. *J. Comp. Physiol. A. Neuroethol. Sens. Neural. Behav. Physiol.* **188**, 211–6.

Dacke, M., Nilsson, D. E., Scholtz, C. H., Byrne, M. and Warrant, E. J. (2003a). Insect orientation to polarized moonlight. *Nature* **424**, 33.

Dacke, M., Nordström, P. and Scholtz, C. H. (2003b). Twilight orientation to polarised light in the crepuscular dung beetle Scarabaeus zambesianus. *J. Exp. Biol.* **206**, 1535–1543.

Dacke, M., Byrne, M. J., Scholtz, C. H. and Warrant, E. J. (2004). Lunar orientation in a beetle. *Proc. R. Soc. B Biol. Sci.* **271**, 361–365.

Dacke, M., Byrne, M. J., Baird, E., Scholtz, C. H. and Warrant, E. J. (2011). How dim is dim? Precision of the celestial compass in moonlight and sunlight. *Philos. Trans. R. Soc. B Biol. Sci.* **366**, 697–702.

Dacke, M., Byrne, M., Smolka, J., Warrant, E. and Baird, E. (2013). Dung beetles ignore landmarks for straight-line orientation. *J. Comp. Physiol. A Neuroethol. Sensory, Neural, Behav. Physiol.* **199**, 17–23.

Eggers, A. and Gewecke, M. (1993). The dorsal rim area of the compound eye and polarization vision in the desert locust (Schistecerca Gregaria). *Sens. Syst. Arthropods. Basel, Switz. Birkhauser* 101–109.

Fortini, M. E. and Rubin, G. M. (1991). The optic lobe projection pattern of polarization-sensitive photoreceptor cells in Drosophila melanogaster. *Cell Tissue Res.* **265**, 185–191.

Foster, J. J., Smolka, J., Nilsson, D. E. and Dacke, M. (2018). How animals follow the stars. *Proc. R. Soc. B Biol. Sci.* **285**,.

Foster, J. J., Kirwan, J. D., el Jundi, B., Smolka, J., Khaldy, L., Baird, E., Byrne, M. J., Nilsson, D. E., Johnsen, S. and Dacke, M. (2019). Orienting to polarized light at night – matching lunar skylight to performance in a nocturnal beetle. *J. Exp. Biol.* **222**,.

Greiner, B., Ribi, W. and Warrant, E. J. (2005). A neural network to improve dim-light vision? Dendritic fields of first-order interneurons in the nocturnal bee Megalopta genalis. *Cell Tissue Res.* **322**, 313–20.

Greiner, B., Cronin, T. W., Ribi, W., Wcislo, W. T. and Warrant, E. J. (2007). Anatomical and physiological evidence for polarisation vision in the nocturnal bee Megalopta genalis. *J. Comp. Physiol. A. Neuroethol. Sens. Neural. Behav. Physiol.* **193**, 591–600.

Hardcastle, B. J., Omoto, J. J., Kandimalla, P., Nguyen, B. C. M., Keleş, M. F., Boyd, N. K., Hartenstein, V. and Frye, M. A. (2021). A visual pathway for skylight polarization processing in drosophila. *Elife* **10**, 1–46.

Hegedüs, R., Horváth, Á. and Horváth, G. (2006). Why do dusk-active cockchafers detect polarization in the green? The polarization vision in Melolontha melolontha is tuned to the high polarized intensity of downwelling light under canopies during sunset. *J. Theor. Biol.* **238**, 230–244.

Heinze, S. (2014). Polarisation Vision. *Encycl. Comput. Neurosci.* 1–30.

Henze, M. J. and Labhart, T. (2007). Haze, clouds and limited sky visibility: Polarotactic orientation of crickets under difficult stimulus conditions. *J. Exp. Biol.* **210**, 3266–3276.

Heras, F. J. H. and Laughlin, S. B. (2017). Optimizing the use of a sensor resource for opponent polarization coding. *PeerJ* **2017**, 1–41.

Herrling, P. L. (1976). Regional Distribution of 3 Ultrastructural Retinula Types in Retina of Cataglyphis-Bicolor Fabr (Formicidae, Hymenoptera). *Cell Tissue Res.* **169**, 247–266.

Herzmann, D. and Labhart, T. (1989). Spectral sensitivity and absolute threshold of polarization vision in crickets: a behavioral study. *J. Comp. Physiol. A* **165**, 315–319.

Homberg, U. and Paech, A. (2002). Ultrastructure and orientation of ommatidia in the dorsal rim area of the locust compound eye. *Arthropod Struct. Dev.* **30**, 271–280.

Homberg, U., Heinze, S., Pfeiffer, K., Kinoshita, M. and el Jundi, B. (2011). Central neural coding of sky polarization in insects. *Philos. Trans. R. Soc. B Biol. Sci.* **366**, 680–687.

Immonen, E. V., Ignatova, I., Gislen, A., Warrant, E., Vähäsöyrinki, M., Weckström, M. and Frolov, R. (2014). Large variation among photoreceptors as the basis of visual flexibility in the common backswimmer. *Proc. R. Soc. B Biol. Sci.* **281**,.

Johnsen, S., Kelber, A., Warrant, E., Sweeney, A. M., Widder, E. A., Lee, R. L. and Hernández-Andrés, J. (2006). Crepuscular and nocturnal illumination and its effects on color perception by the nocturnal hawkmoth Deilephila elpenor. *J. Exp. Biol.* **209**, 789–800.

Khaldy, L., Foster, J. J., Yilmaz, A., Belušič, G. and Gagnon, Y. (2022). The interplay of directional information provided by unpolarised and polarised light in the heading direction network of the diurnal dung beetle Kheper lamarcki. *J. Exp. Biol.* **225**,.

Kind, E., Longden, K. D., Nern, A., Zhao, A., Sancer, G., Flynn, M. A., Laughland, C. W., Gezahegn, B., Ludwig, H. D. F., Thomson, A. G., et al. (2021). Synaptic targets of photoreceptors specialized to detect color and skylight polarization in Drosophila. *Elife* **10**, 1–48.

Klaus, A. and Warrant, E. J. (2009). Optimum spatiotemporal receptive fields for vision in dim light. *J. Vis.* **9**,.

Labhart, T. (1980). Specialized photoreceptors at the dorsal rim of the honeybee's compound eye: Polarizational and angular sensitivity. *J. Natl. Cancer Inst.* **141**, 19–30.

Labhart, T. (1986). The electrophysiology of photoreceptors in different eye regions of the desert ant, Cataglyphis bicolor. *J. Comp. Physiol. A* **158**, 1–7.

Labhart, T. (1999). How polarization-sensitive interneurones of crickets see the polarization pattern of the sky: A field study with an optoelectronic model neurone. *J. Exp. Biol.* **202**, 757–770.

Labhart, T. and Meyer, E. P. (1999). Detectors for polarized skylight in insects: A survey of ommatidial specializations in the dorsal rim area of the compound eye. *Microsc. Res. Tech.* **47**, 368–379.

Labhart, T., Hodel, B. and Valenzuela, I. (1984). The physiology of the cricket's compound eye with particular reference to the anatomically specialized dorsal rim area. *J. Comp. Physiol. A* **155**, 289–296.

Labhart, T., Meyer, E. P. and Schenker, L. (1992). Specialized ommatidia for polarization vision in the compound eye of cockchafers, Melolontha melolontha (Coleoptera, Scarabaeidae). *Cell Tissue Res.* **268**, 419–429.

Labhart, T., Petzold, J. and Helbling, H. (2001). Spatial integration in polarization-sensitive interneurones of crickets: a survey of evidence, mechanisms and benefits. *J. Exp. Biol.* **204**, 2423–30.

Labhart, T., Baumann, F. and Bernard, G. D. (2009). Specialized ommatidia of the polarization-sensitive dorsal rim area in the eye of monarch butterflies have non-functional reflecting tapeta. *Cell Tissue Res.* **338**, 391–400.

Land, M. F. (1997). Visual acuity in insects. *Annu. Rev. Entomol.* **42**, 147–177.

Loesel, R. and Homberg, U. (2001). Anatomy and physiology of neurons with processes in the accessory medulla of the cockroach Leucophaea maderae. *J. Comp. Neurol.* **439**, 193–207.

Mathejczyk, T. F. and Wernet, M. F. (2017). Sensing Polarized Light in Insects. *Oxford Res. Encycl. Neurosci.* 1–31.

Meyer-Rochow, V. B. (1981). Electrophysiology and histology of the eye of the bumblebee Bombus hortorum (L.) (Hymenoptera: Apidae). *J. R. Soc. New Zeal.* **11**, 123–153.

Muheim, R., Phillips, J. B. and Deutschlander, M. E. (2009). White-throated sparrows calibrate their magnetic compass by polarized light cues during both autumn and spring migration. *J. Exp. Biol.* **212**, 3466–3472.

Nilsson, D. E. and Howard, J. (1989). Intensity and polarization of the eyeshine in butterflies. *J. Comp. Physiol. A* **166**, 51–56.

Nilsson, D. E., Labhart, T. and Meyer, E. (1987). Photoreceptor design and optical properties affecting polarization sensitivity in ants and crickets. *J. Comp. Physiol. A* **161**, 645–658.

Novales Flamarique, I. (2019). Swimming behaviour tunes fish polarization vision to double prey sighting distance. *Sci. Rep.* **9**, 1–8.

Peirce, J., Gray, J. R., Simpson, S., MacAskill, M., Höchenberger, R., Sogo, H., Kastman, E. and Lindeløv, J. K. (2019). PsychoPy2: Experiments in behavior made easy. *Behav. Res. Methods* **51**, 195–203.

Pomozi, I., Horváth, G. and Wehner, R. (2001). How the clear-sky angle of polarization pattern continues underneath clouds: Full-sky measurements and implications for animal orientation. *J. Exp. Biol.* **204**, 2933–2942.

Reid, S. F. (2010). Life in the dark: Vision and navigation in a nocturnal bull ant.

Rossel, S. and Wehner, R. (1984). Celestial orientation in bees: the use of spectral cues. *J. Comp. Physiol. A* **155**, 605–613.

Rossel, S., Wehner, R. and Lindauer, M. (1978). E-Vector orientation in bees. *J. Comp. Physiol. A* **125**, 1–12.

Sancer, G., Kind, E., Plazaola-Sasieta, H., Balke, J., Pham, T., Hasan, A., Münch, L. O., Courgeon, M., Mathejczyk, T. F. and Wernet, M. F. (2019). Modality-Specific Circuits for Skylight Orientation in the Fly Visual System. *Curr. Biol.* **29**, 2812-2825.e4.

Schmeling, F., Wakakuwa, M., Tegtmeier, J., Kinoshita, M., Bockhorst, T., Arikawa, K. and Homberg, U. (2014). Opsin expression, physiological characterization and identification of photoreceptor cells in the dorsal rim area and main retina of the desert locust, Schistocerca gregaria. *J. Exp. Biol.* **217**, 3557–3568.

Seidl, T., Knaden, M. and Wehner, R. (2006). Desert ants: is active locomotion a prerequisite for path integration? *J. Comp. Physiol. A. Neuroethol. Sens. Neural. Behav. Physiol.* **192**, 1125–31.

Seliger, H. H., Lall, A. B. and Biggley, W. H. (1994). Blue through UV polarization sensitivities in insects - Optimizations for the range of atmospheric polarization conditions. *J. Comp. Physiol. A* **175**, 475–486.

Sharkey, C. R., Fujimoto, M. S., Lord, N. P., Shin, S., McKenna, D. D., Suvorov, A., Martin, G. J. and Bybee, S. M. (2017). Overcoming the loss of blue sensitivity through opsin duplication in the largest animal group, beetles. *Sci. Rep.* **7**, 1–10.

Stalleicken, J., Labhart, T. and Mouritsen, H. (2006). Physiological characterization of the compound eye in monarch butterflies with focus on the dorsal rim area. *J. Comp. Physiol. A Neuroethol. Sensory, Neural, Behav. Physiol.* **192**, 321–331.

Theobald, J. C., Coates, M. M., Wcislo, W. T. and Warrant, E. J. (2007). Flight performance in night-flying sweat bees suffers at low light levels. *J. Exp. Biol.* **210**, 4034–4042.

Tocco, C., Dacke, M. and Byrne, M. (2019). Eye and wing structure closely reflects the visual ecology of dung beetles. *J. Comp. Physiol. A Neuroethol. Sensory, Neural, Behav. Physiol.* **205**, 211–221.

Tocco, C., Dacke, M. and Byrne, M. (2021). The finely defined shift work schedule of dung beetles and their eye morphology. *Ecol. Evol.* **11**, 15947–15960.

Warrant, E. J. and McIntyre, P. D. (1991). Strategies for retinal design in arthropod eyes of low F-number. *J. Comp. Physiol. A* **168**, 499–512.

Warrant, E. J. and Nilsson, D. E. (1998). Absorption of white light in photoreceptors. *Vision Res.* **38**, 195–207.

Wehner, R. and Müller, M. (2006). The significance of direct sunlight and polarized skylight in the ant's celestial system of navigation. *Proc. Natl. Acad. Sci. U. S. A.* **103**, 12575–12579.

Weir, P. T. and Dickinson, M. H. (2012). Flying drosophila orient to sky polarization. *Curr. Biol.* **22**, 21–27.

Wernet, M. F., Labhart, T., Baumann, F., Mazzoni, E. O., Pichaud, F. and Desplan, C. (2003). Homothorax switches function of Drosophila photoreceptors from color to polarized light sensors. *Cell* **115**, 267–279.

Wernet, M. F., Velez, M. M., Clark, D. A., Baumann-klausener, F., Brown, J. R., Klovstad, M., Labhart, T. and Clandinin, T. R. (2012). Genetic dissection reveals two separate retinal substrates for polarization vision in Drosophila. *Curr. Biol.* **22**, 12–20.

Wu, M., Bao, R. and Friedrich, M. (2020). Evolutionary conservation of opsin gene expression patterns in the compound eyes of darkling beetles. *Dev. Genes Evol.* **230**, 339–345.

Wunderer, H. and Smola, U. (1982). Fine structure of ommatidia at the dorsal eye margin of Calliphora erythrocephala meigen (Diptera: Calliphoridae): An eye region specialised for the detection of polarized light. *Int. J. Insect Morphol. Embryol.* **11**, 25–38.

Yilmaz, A., el Jundi, B., Belušič, G., Marcus, B., Baird, E. and Dacke, M. (2022). Mechanisms of spectral orientation in a diurnal dung beetle. *Philos. Trans. B* **377**,.

Zufall, F., Schmitt, M. and Menzel, R. (1989). Spectral and polarized light sensitivity of photoreceptors in the compound eye of the cricket (Gryllus bimaculatus). *J. Comp. Physiol. A* **164**, 597–608.

Figures

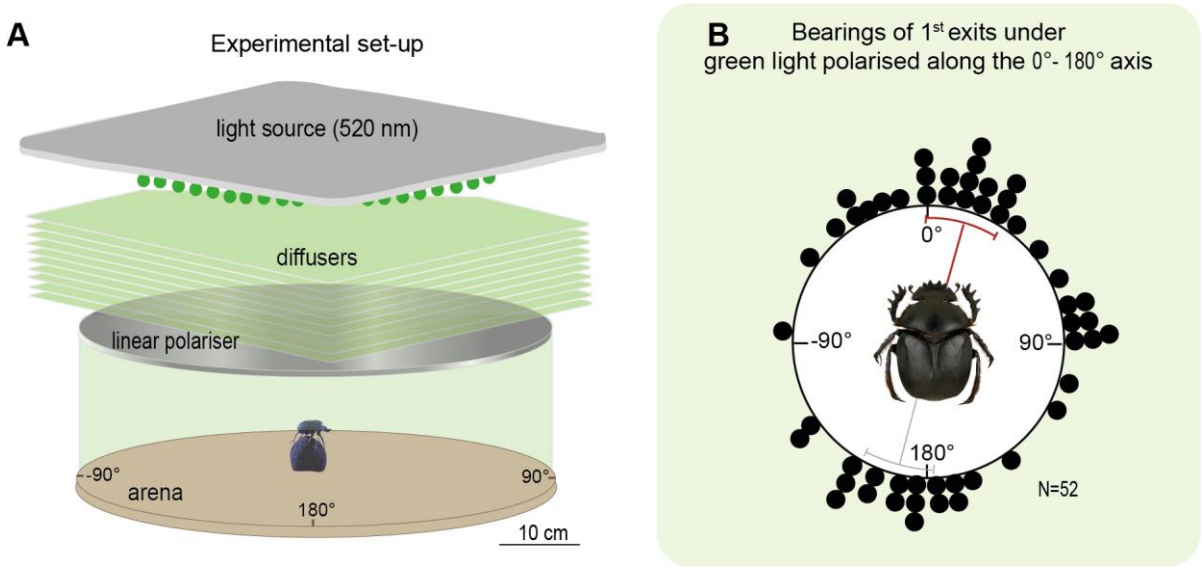

Fig. 1. Experimental set-up and distribution of first exit bearings. (A) An LED array, a stack of diffusers, and a linear polariser provided the beetles with uniform and highly polarised green overhead light. Each beetle rolled its ball from the centre to the edge of the arena, where its exit angle was noted. **(B)** Distribution of the first exit bearings of the beetles (n=52). The beetles preferentially exited the arena in directions that aligned with the e-vector of light i.e. along the 0-180° axis. Mean angles are shown in red and grey lines, red and grey sectors show 95% confidence interval of the mean.

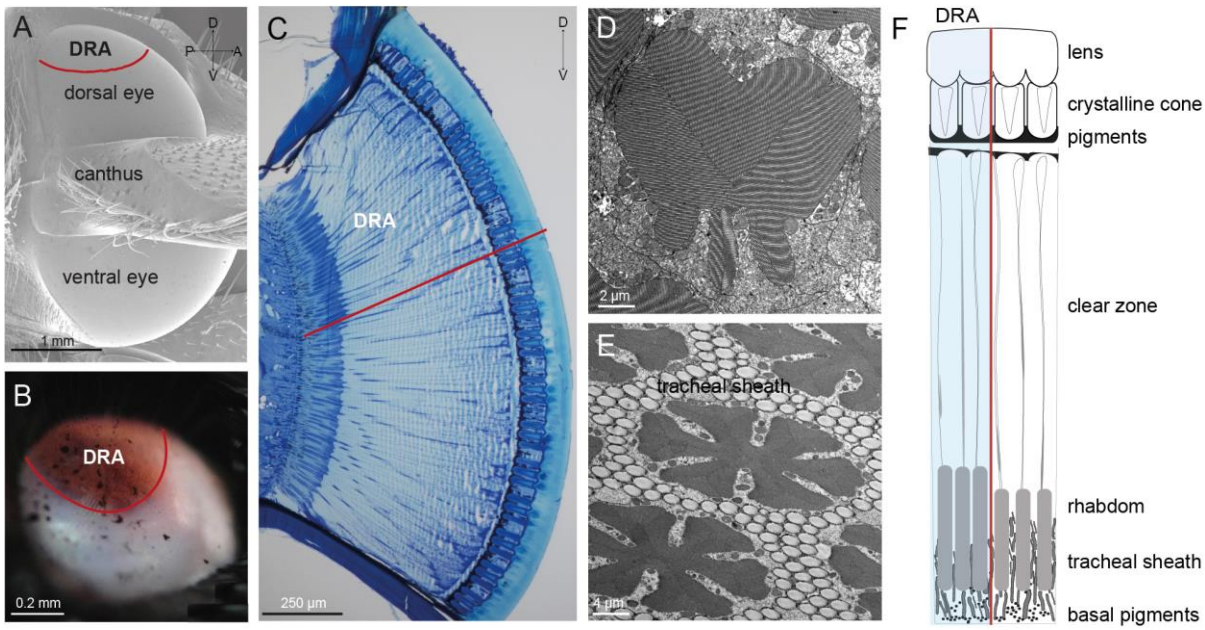

Fig. 2. Morphology of the eye of *Escarabaeus satyrus*. (A) The canthus separates the eye into a dorsal and a ventral part (adapted from (Tocco et al., 2019)). The region of polarisation sensitive photoreceptors (DRA) is located in the upper part of the dorsal eye. **(B)** After removal of the distal elements of the eye, the DRA retina appears darker and redder than the main retina. This is likely due to the relatively shorter reflective tracheal sheath in the DRA retina. **(C)** Longitudinal and **(D)** cross sections of the dorsal eye with relatively longer and heart-shaped rhabdoms in the DRA retina**. (E)** Flower shaped rhabdom in the main retina are surrounded by tracheal sheath. **(F)** Schematic with the elements of the DRA (light blue) and the main dorsal eye. D: dorsal, V:ventral, A:anterior, P:posterior. Red line (A-C, F) indicates the approximate separation between the DRA and the main retina.

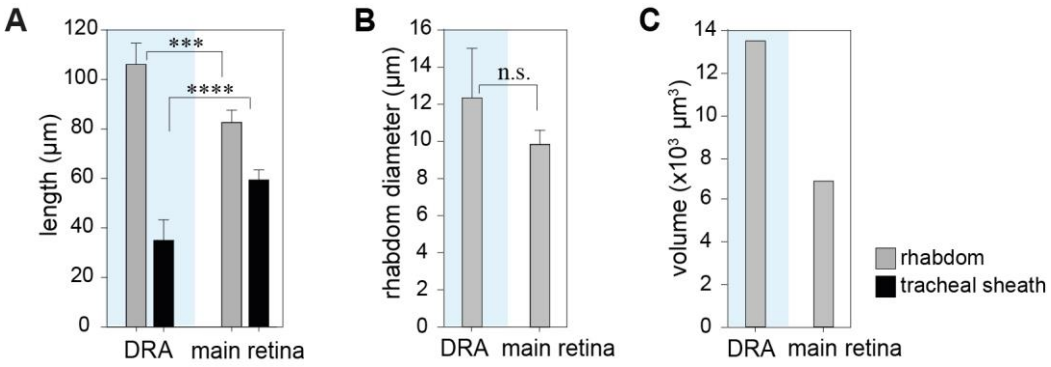

Fig. 3. Comparison of rhabdom characteristics in the DRA (light blue) and the main retina. (A) The rhabdoms in the DRA are significantly longer than those of the main retina (t-test, $p < 0.001$, n=9), while the reverse is true for the reflective tracheal sheath that partly surrounds the rhabdoms (t-test, $p < 0.0001$). (B, C) As there are no significant differences in rhabdom diameters across the eye (t-test, $p > 0.05$), the resulting rhabdomeric volumes in the DRA (approximated as a cylindrical shape) are larger than those in the rest of the eye.

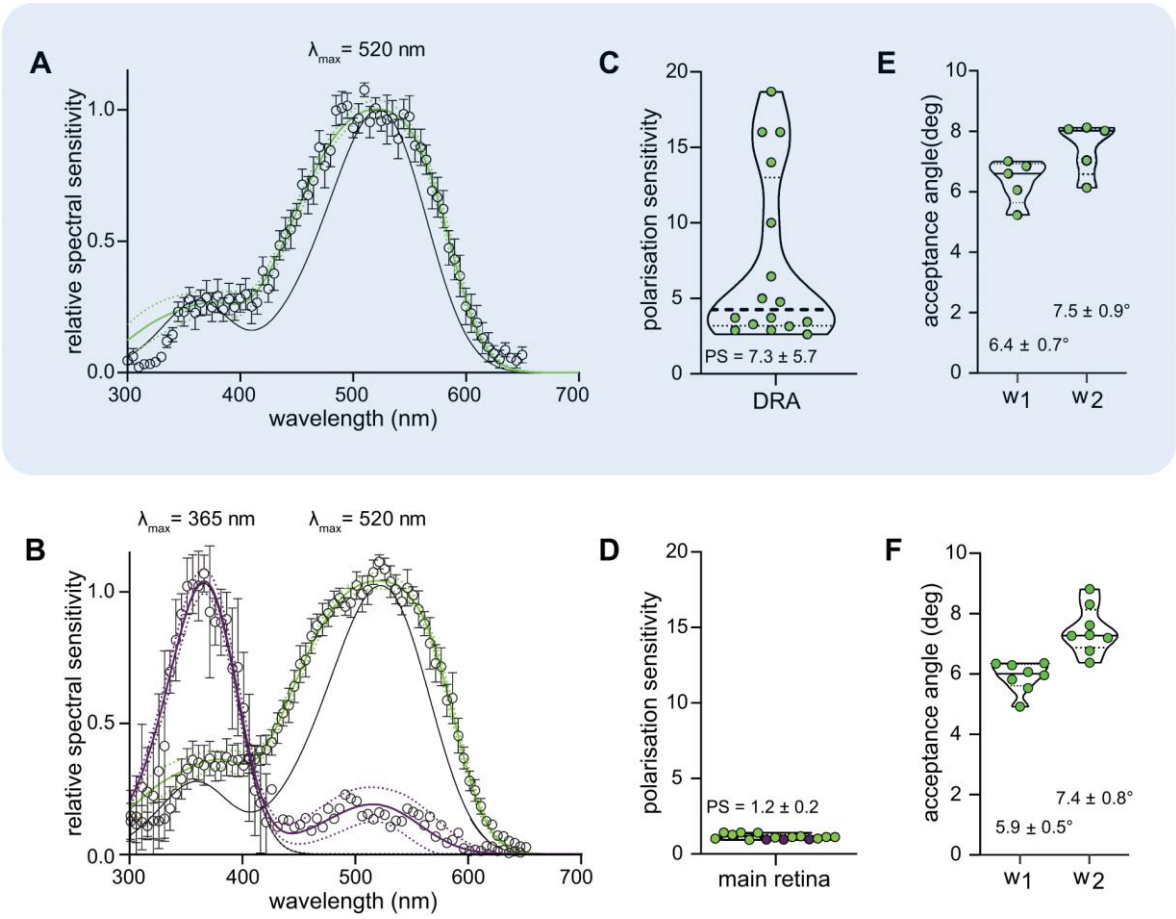

Fig. 4. Intracellular photoreceptor recordings in the dorsal eye of *Escarabaeus satyrus*. **(A)** Photoreceptors in the dorsal rim area (DRA) are maximally sensitive to the green range of the spectrum (λmax ≈ 520 nm, n= 7). **(B)** Photoreceptors in the main retina are of two types, one maximally sensitive to the green (λmax ≈ 520 nm, n=8) and one maximally sensitive to the UV (λmax ≈ 365 nm, n=3) range of the spectrum. Measured spectral sensitivities (open data points with error bars, mean ± SE) are fitted to rhodopsin absorbance templates (black curves) and corrected for self-screening (green and violet curves). Dotted curves (green and violet) represent the upper and lower values of the standard error of the fit. **(C)** DRA photoreceptors are polarisation sensitive. **(D)** Main retina photoreceptors are not polarisation sensitive. Green data points in in **(C)** and green and purple data points in (**D)** represent polarisation sensitivities of green- and UV-sensitive cells, respectively. **(E, F)** The oval-shaped receptive fields (described with two angular radii, W_1 and W_2) of the green-sensitive DRA photoreceptors are only slightly larger than those of the green-sensitive photoreceptors in the main retina. Acceptance angles and polarisation sensitivities are given as mean ± SE. Dashed and dotted lines indicate median and first and third quartile of the data.

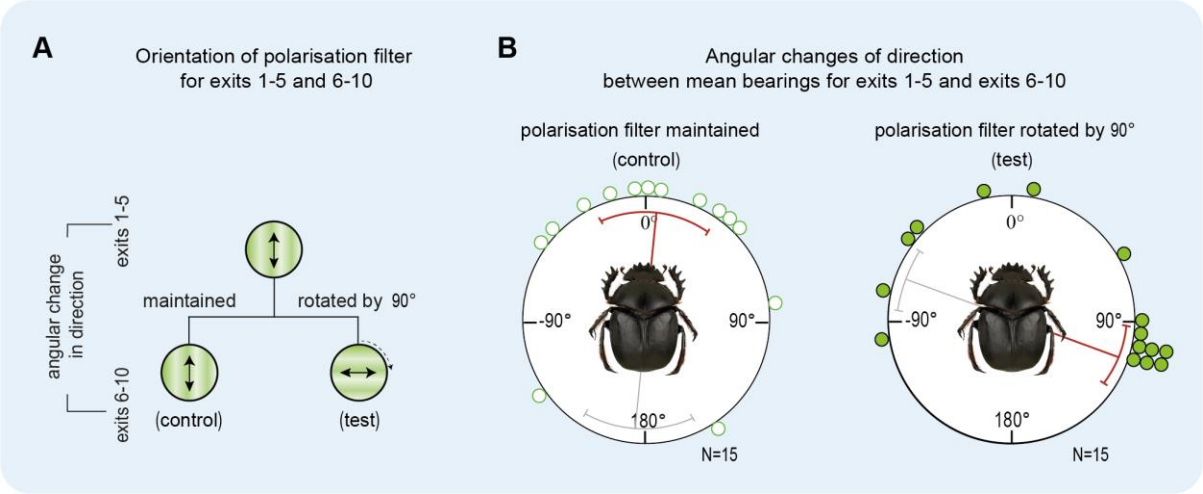

Fig. 5. A clear orientation response of *Escarabaeus satyrus* to green polarised overhead light. (A) When a beetle had exited the experimental arena (see Fig 1a) five times, the overhead linear polariser was either maintained in position (*control*) or rotated by 90° (*test*). The beetle was then allowed to exit the arena another five times. Angular change of direction was calculated as the difference between the mean bearing for exits 1-5 and the mean bearing for exits 6-10. **(B)** When the polariser was maintained in position (*control*), angular changes of direction were clustered along the 0°-180° axis, i.e the beetles did not change their bearings. When the polariser was instead rotated by 90° (*test*), the angular changes of direction were clustered along the 90° to -90° axis, i.e the beetles changed their bearings in response to the rotated polariser. Mean angles are represented by red and grey lines, red and grey sectors show 95% confidence interval of the mean.

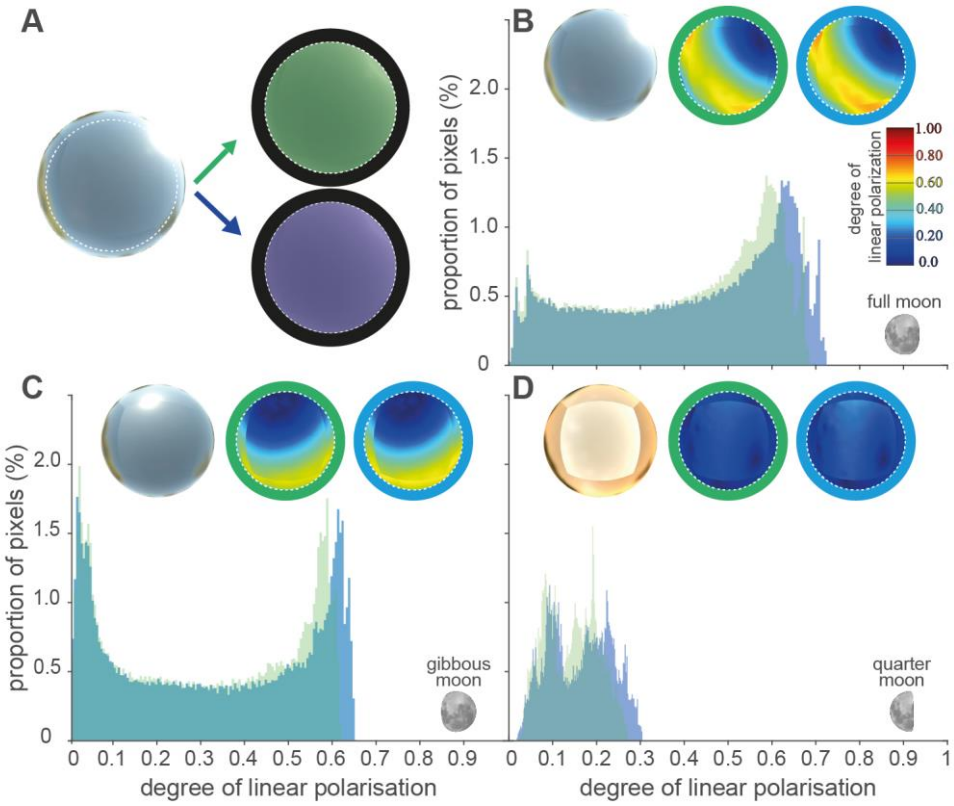

Fig. 6. Measurements of polarised skylight. **(A)** Spherical images were filtered with a 7° full-width at half-maximum gaussian to simulate the receptive fields of the DRA photoreceptors. The resulting radiance profiles, shown here as a fisheye projection facing upwards towards the zenith (dashed line indicates 30°), were split into the camera's "blue" (short wavelength) and "green" (longer wavelength) channels, retaining only pixels above 30° of elevation clear of all surrounding vegetation. Inset images in (**B**), (**C**) and **(D)** show the RGB linearised radiance of the filtered sky (left), and the degree of polarization in the green (middle) and blue (right) channels. The degrees of polarisation measured for each camera pixel are shown as overlaid histograms for the camara's green (green shaded area) and blue (blue shaded area) channels. (**B**) A waxing gibbous moon close to full moon (98% illuminated) at a low elevation. There is a notable shift towards lower degrees of polarisation for the green channel as compared to the blue channel. **(C)** A waning gibbous moon (93% illuminated) at a higher elevation. **(D)** A moonlit sky at moonset during first quarter (49% illuminated). In this case the modal degree of polarization for the green channel (around 0.15) is close to the reported threshold for *E. satyrus*. Skylight polarisation data was adapted from (Foster et al., 2019).

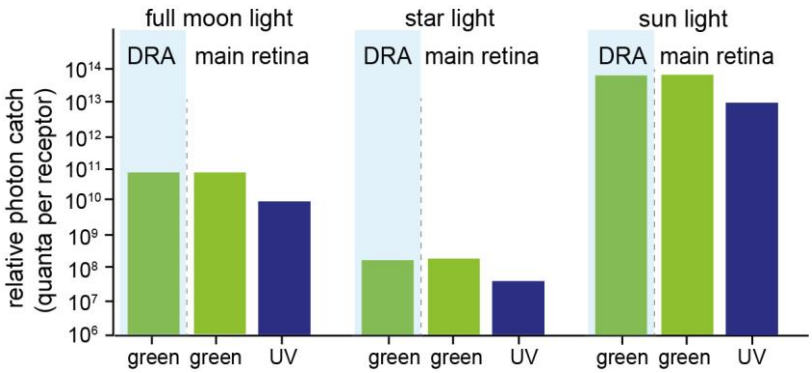

Fig. 7. Photon catch calculations for UV- and green-sensitive photoreceptors in the dorsal rim area (DRA) and the main retina. Recorded relative spectral sensitivities and irradiance spectra reported by Johnsen et al., (2006) were used to calculate the relative photon catch of green-sensitive photoreceptors in the DRA and green- and UV- sensitive photoreceptors in the main retina. In moonlit, starlit, and sunlit conditions, the green-sensitive photoreceptors catch an order of magnitude more photons compared to the UV-sensitive photoreceptors.